# Charging a Smartphone Across a Room Using Lasers

VIKRAM IYER*, ELYAS BAYATI*, RAJALAKSHMI NANDAKUMAR, ARKA MAJUMDAR, and SHYAMNATH GOLLAKOTA, University of Washington, USA

We demonstrate a novel laser-based wireless power delivery system that can charge mobile devices such as smartphones across a room. The key challenges in achieving this are multi-fold: delivering greater than a watt of power across the room, minimizing the exposure of the resulting high-power lasers to human tissue, and finally, ensuring that the design meets the form-factor requirements of a smartphone and requires minimal instrumentation to the environment. This paper presents a novel, and to the best of our knowledge, the first design, implementation and evaluation of an end-to-end power delivery system that satisfies all the above requirements. Our results show that we can deliver more than 2 W at ranges of 4.3 m and 12.2 m for a smartphone ($25\ cm^2$) and table-top form factor ($100\ cm^2$) receiver respectively. Further, extensive characterization of our safety system shows that we can turn off our laser source much before a human moving at a maximum speed of 44 $m/s$ can even enter the high-power laser beam area.

CCS Concepts: • **Hardware** → **Communication hardware, interfaces and storage**; • **Human-centered computing** → *Ubiquitous and mobile computing*;

Additional Key Words and Phrases: Wireless power; Optics; Retroreflectors; Optical Backscatter; Acoustic Localization

## 1 INTRODUCTION

Wireless access has become a fundamental part of daily life with the growing ubiquity of smartphones and other mobile devices all around us. While wireless communication techniques have untethered mobile devices, wireless power transfer still remains an unsolved problem. Recent advances in near-field wireless charging techniques have begun to gain traction for certain range-limited applications including cars, drones, and cell phone charging mats [12]. At the same time, a growing body of work focused on energy harvesting from ambient RF signals such as Wi-Fi, cellular base stations, and TV signals [24, 44] is enabling ultra-low power battery-free devices. Near-field systems provide a good solution for high power systems at close ranges, while RF harvesting allows for long-range operation at a very low power. This however leaves open a significant need for a wireless power solution that can enable truly untethered applications that require both high power and long ranges.

In this paper, we ask the following question: can we design a system that wirelessly transfers power across a room to charge mobile devices such as smartphones? A positive answer would enable scenarios where one could

---

*Co-primary Student Authors

Authors' address: Vikram Iyer; Elyas Bayati; Rajalakshmi Nandakumar; Arka Majumdar;
Shyamnath Gollakota, University of Washington, 185 Stevens Way, Seattle, WA, 98195, USA, {vsiyer,elyasb,rajaln,arka,gshyam}@uw.edu.

(a) Charging a smartphone.     (b) Charging a camera     (c) Delivering power to a tabletop
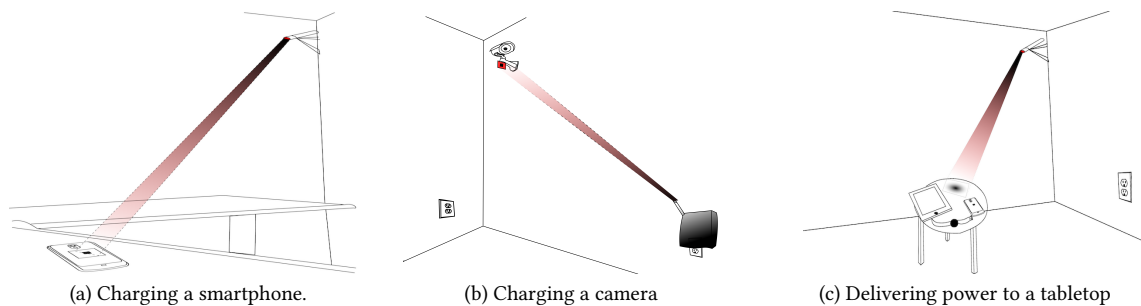
Fig. 1. **Applications for our laser power delivery system.** It can be used to charge smartphones as well as IoT sensors and devices including Wi-Fi cameras across a room. It can also be used to deliver power to a tabletop that is far away from wall outlets, which can in turn charge mobile devices placed on it.

imagine a phone automatically charging when placed on a table anywhere within a room. This would eliminate the hassle of finding a charging cable and power outlet, or for example forgetting to plug it in overnight. One could also imagine extending this concept to transfer power to a whole table top. For instance, a coffee table in the center of a room away from wall outlets could now have wireless power access, which can in turn charge mobile devices placed on it. This can also enable wireless power to battery-free sensors as well as home and industrial automation devices such as Wi-Fi HD streaming cameras shown in Fig. 1 that currently have to be plugged in.

Designing a wireless power system capable of charging a device like a smartphone across a room is however not trivial, and requires satisfying the three key requirements we outline below:

(1) *Deliver greater than 1 W across a room.* The USB 2.0 standard allows for 1–2.5 W of power [10]. We would like to achieve this across at least a 5 m room to be practical. Further, in order to make such a system economical, a wireless power system should be designed to operate efficiently.

(2) *Is safe for consumer user.* When transmitting high power wireless signals across a room, safety is paramount. High power electromagnetic and acoustic waves are harmful to the human body [22, 39] and governments define strict exposure rules for commercial products to ensure user safety.

(3) *Meets form-factor requirements and requires minimal instrumentation.* In order to make a wireless power system practical for deployment, it should have minimal instrumentation. Ideally, we would like a system that does not require adding significant infrastructure beyond a single transmitter and receiver. Additionally, the form factor of the receiver should be within the dimensions of a commodity smartphone to allow for integration into a case, or eventually into mobile devices themselves.

In this paper, we present a novel, and to the best of our knowledge, the first design, implementation and evaluation of an end-to-end wireless power delivery system that satisfies all the above requirements. To achieve this we use near-infrared lasers to deliver power safely across a room. Unlike near-field systems, lasers can operate over long distances with minimal attenuation since they provide a highly focused beam with high power density. Further, lasers and photovoltaic cells can easily operate at powers exceeding a few watts.

The challenge however is in ensuring safety while using a high power laser. Delivering 1 W of power to a 1 cm$^2$ receiver with 23% efficiency requires a power density greater than 4.3 $W/cm^2$. This presents a serious safety concern as lasers in the visible and near-IR wavelength range at this power level can cause damage to the eye when exposed for less than 10 $\mu$s. A naïve solution is to detect a reduction in the received power whenever a human enters the laser beam and send feedback back to the laser source to turn off the beam. This is however difficult for two key reasons. First, sending feedback via Wi-Fi or other existing radio mechanisms introduces a significant delay on the order of a few milliseconds, which is orders of magnitude more than the permissible

exposure time. Second, even if one can turn off the power to the laser immediately, commodity continuous wave laser drivers have control circuits that may introduce significant delays. For example, the interlock of the MHGoPower LSM-010 laser has a delay of 272 $\mu$s.

In this paper, we design a novel safety solution and provide extensive characterization supported by empirical data to show that our design will never expose a human to the high power laser and yet can deliver more than a watt to a smartphone form-factor receiver. Our key idea is to use a backscatter approach: measure the reflected light from the receiver directly at the laser source. Specifically, we use a series of retroreflectors at the receiver. A retroreflector is an optical element that reflects light back in the same direction from which it arrived unlike a typical flat mirror. We create a low-power guard beam around the high power laser and use retroreflectors at the receiver to reflect this guard beam. By directing a guard ring of low power lasers from the laser source at these passive optical elements at the receiver, we can measure its reflection directly at the laser source using photodiodes. In order to receive a reflection, we must have line of sight to the retroreflector at the receiver, and any motion that blocks the low-power guard beam will propagate back to the photodiode at the speed of light. Since the roundtrip for an optical reflection at a distance of 10 m is only 60 ns and photodiodes can easily operate at nanosecond speeds [34], this approach allows us to build a motion detection system that operates on the order of nanoseconds. By appropriately picking the diameter of the guard beam, we account for the delay in turning off the high power beam and ensure that living tissue never gets in the path of the high power laser beam.

In addition to the safety concerns, our design also addresses other practical issues including localization and heating effects. Specifically, we introduce two additional techniques:

- *Joint acoustic and optical localization.* We show how to use an acoustic localization system to locate the receiver to a coarse level prior to finer alignment using the retroreflectors and initiating high power transfer. By using acoustic localization we allow the receiver to indicate that it is ready to receive power, and further prevent the need to scan across the whole room using our low power lasers to find the receiver.
- *Form-factor heat energy harvesting.* We design a receiver fully compatible with the form factor of a smartphone including a heatsink. Delivering high power to the photovoltaic (PV) cells can quickly increase their temperature up to 150°C at which point they can only remain operational for a few seconds. We design a form factor heat sink that not only cools down the system to prevent this problem but also uses a thermoelectric generator to harvest up to 5 mW from the wasted heat generated by the PV cell.

We implement a prototype of our design using commodity optical components including the MHGoPower LSM-010 976 nm laser source. Since commodity retroreflectors have a limited field of view and large form factor, we designed and fabricated our own corner cube reflectors that can operate across a wide range of angles. Our results show that we can wirelessly transmit 1 W of useful power at ranges up to 3.6 m using a single 1 $cm^2$ PV cell. Using an array of photocells, this translates to delivering more than 2 W of power at ranges of 4.3 m and 12.2 m for a smartphone (25 $cm^2$) and table-top form factor (100 $cm^2$) receiver respectively. We perform extensive characterization of our safety system showing that we can turn off our high power laser before a human moving with a maximum speed of 44 m/s can enter the high power beam area. Additionally we demonstrate the full system beginning with a novel acoustic localization system to our low profile heatsink and thermoelectric generator which allow for a stable 1.3 W output for over eight hours from single PV cell.

## 2 A CASE FOR OUR APPROACH

Traditional approaches to wireless power include near-field magnetic induction, far field microwave approaches, and optical systems. In order to motivate our solution, we analyze each of these techniques in detail below to explore their trade offs and evaluate whether they meet the requirements for our wireless power system.

**Magnetic induction.** Perhaps the most commercially successful wireless power transfer technology is near-field magnetic induction. This method typically involves two coupled resonators that transfer power between each

other at close range. This is the technique that has been adopted by the Qi wireless charging standard and has seen adoption into commercial Samsung smartphones as well as charging mats. Additionally, this method is being explored for wirelessly charging cars, drones etc. [12, 45]. While this method is safe and efficient it is fundamentally limited in terms of range to tens of centimeters in practice. Specifically, these systems can operate efficiently up to distances on the order of the coils' diameter, but decreases dramatically beyond this point [19]. Recent work has demonstrated methods of improving this range by using relay coils [26]. While adding additional coils between the transmitter and receiver addresses range, it requires setting up significant additional instrumentation in the path between the transmitter and receiver. Similarly [6] proposes transforming an entire room into a resonant cavity. While, this addresses the problem of range within a room, it also requires significant infrastructure changes to the whole room.

**Far Field RF.** Power harvesting from far field microwave sources has received much attention in recent years and a variety of works have demonstrated harvesting small amounts of power from sources like Wi-Fi [44], TV signals [24, 33] and RFID readers [5, 7]. However these approaches are only suitable for ultra-low power applications that require only a few micro-watts to operate. These ambient power harvesting methods suffer from the fact that existing communication signals are designed to be broadcast over a wide area rather than for focused transmission of power to a specific device.

Achieving power transfer greater than 1 W therefore requires a dedicated power transmitter. While increasing transmit power can increase the amount of power at the receiver, this raises a host of other problems. First, the efficiency of this approach is fundamentally limited by path loss in free space. If we take the example of a system operating at 2.4 GHz, the ratio of transmitted RF power to the RF power available to a receiver at distance $d$ assuming no additional losses is given by, $\frac{P_r}{P_t} = G_t G_r \left(\frac{\lambda}{4\pi d^2}\right)$. Assuming we wish to transfer power at a distance of 5 m with a receiver antenna gain of 0 dBi at the smartphone, we plot the required transmit power to receive 1 W of RF power for different transmit antenna gains in Fig. 2. We also plot the efficiency of this link as the percentage of RF power from the transmitter available at the receiver. This plot shows that even with a highly directional 30 dBi large antenna (or phased arrays), the required transmit power exceeds 1.2 kW achieving an efficiency of only 0.8%. This efficiency number does not include the additional losses in RF to DC conversion. Although it is physically possible to design higher gain antennas at 2.4 GHz using a large radius dish, this becomes impractical for indoor uses[1]. Based on this analysis, RF power transfer does not meet our efficiency criteria.

Second, this approach would also violate safety regulations. The maximum RF power density allowed by the FDA is 1 $mW/cm^2$. Smartphones typically have an area of 100-130 $cm^2$, which presents a trade off between meeting the power density limits for safety and desired form factor. Even assuming an antenna array could efficiently harvest all of the energy over the area on a phone, the maximum RF power available would be limited to 130 mW. While startups in recent years [9, 18] have proposed large antenna arrays capable of beamforming power to a receiver, we believe these approaches would have a hard time providing safety guarantees since there would be points of constructive interference from the complex multipath in indoor environments that exceed safe power limits. Considering multipath will also vary in different environments, it would be difficult to guarantee safety in all cases using far field RF based approaches.

Finally, microwave power transmission systems operating in the ISM band would disrupt existing communications such as Wi-Fi and cellular. Since all real transmitters have some amount of phase noise, a high power transmitter even in a *different* Wi-Fi channel could still impact throughput. To demonstrate this, we perform a simple experiment in which we configure a USRP and power amplifier (RFMD PA5201E-410) to transmit a 28 dBm single tone signal to a 15 dBi parabolic reflector antenna resulting in a received RF power of 0.01 W at a Wi-Fi receiver antenna. We run an iperf throughput measurement between a WRT54G Wi-Fi router and an

---

[1]Going to millimeter wave frequencies can reduce the antenna size, however mm wave power amplifiers at tens of Watts become more complex, expensive, and less power efficient
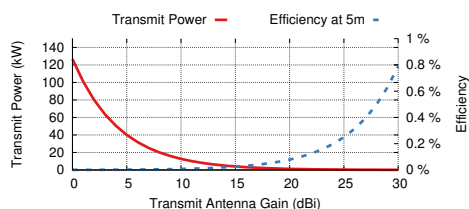
Fig. 2. **RF charging efficiency.** RF charging requires transmitting kilowatts of power to receive 1 W at a receiver. Even with a 30 dBm high gain transmit antenna, the power transfer efficiency is less then 0.8%.
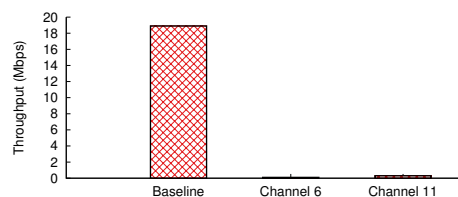


Fig. 3. **Impact of RF power on Wi-Fi throughput**. The plot shows Wi-Fi throughput at the receiver on channel 1 during high power transmissions directed at the same receiver in adjacent Wi-Fi channels 6 and 14.

Intel 7260 laptop Wi-Fi card (which is our receiver) each with 3 dbi monopole antenna on Wi-Fi channel 1, and test the effect of transmitting high power out of band interference on the neighboring Wi-Fi channels 6 and 11. We plot the results as well as a baseline throughput measurement with no adjacent-band power transmission. Fig. 3 demonstrates that even with a significant frequency separation, our channel 1 Wi-Fi throughput drops to 70 Kbps. Independent of the safety concerns, transmitting high power signals in the ISM bands to a phone would severely affect the phone's ability to communicate via Wi-Fi.

**Optical charging.** While there is a large body of work on components for laser systems such as high efficiency photovoltaic cells [35] and laser sources, we focus on works that present end-to-end power delivery systems.

Some of the earliest works on laser based power come from research on space based solar power which aims to harvest solar energy and beam it down to ground stations on earth or space exploration vehicles [14]. Research efforts by the US Navy and DoD have proposed similar systems that operate in reverse using ground stations to power satellites [4]. Laser power systems have also been proposed for a variety of space exploration applications such as space elevators [21] and rovers [30, 42]. Additionally, there has been recent interest in laser power for UAVs [1, 29, 31]. Other works have also proposed laser based power for structural health sensors on bridges [20]. While these systems demonstrate the potential of laser based wireless power, they focus on applications in outdoors and environments where safety is not a primary concern.

[27] demonstrates a laser and photovoltaic cell capable of operating at higher optical wavelengths, however this is a preliminary work that does not develop a full end-to-end power delivery solution. [37] demonstrates a 1410 nm system capable of transmitting 0.59 W at a range of 4 m. The authors mention that the laser could be turned off upon detecting a drop in received power, but do not describe the method for transmitting this information back to the laser source within the time constraints required for safety. In contrast we present the design and implementation of an optical backscatter system that detects a person and turns off the laser before a human ever interacts with the high power beam. Finally [25] uses a high intensity visible light similar in intensity to bright sunlight to transmit power to a solar cell connected to a phone. This work uses a 30 fps camera to detect humans but requires a large delay of 50 ms. In addition to using high-intensity visible light which is not desirable in practice, the use of a diverging light beam rather than a laser presents a similar challenge to RF for achieving high efficiency at longer ranges and different angles. In contrast to these works, we provide the first rigorous characterization of a full laser power transmission system including our novel retroreflector based safety system and acoustic localization techniques. We demonstrate this system is capable of operating over a range of angles and ranges and develop a prototype in a form factor compatible with charging a smartphone.

A recent work on WiCharge proposes an alternative optical wireless power method which aims to transform the space between the transmitter and receiver itself into the resonant cavity that produces a high power laser [23]. In this method, a cavity is claimed to be formed between two retroreflectors separated by the distance over which
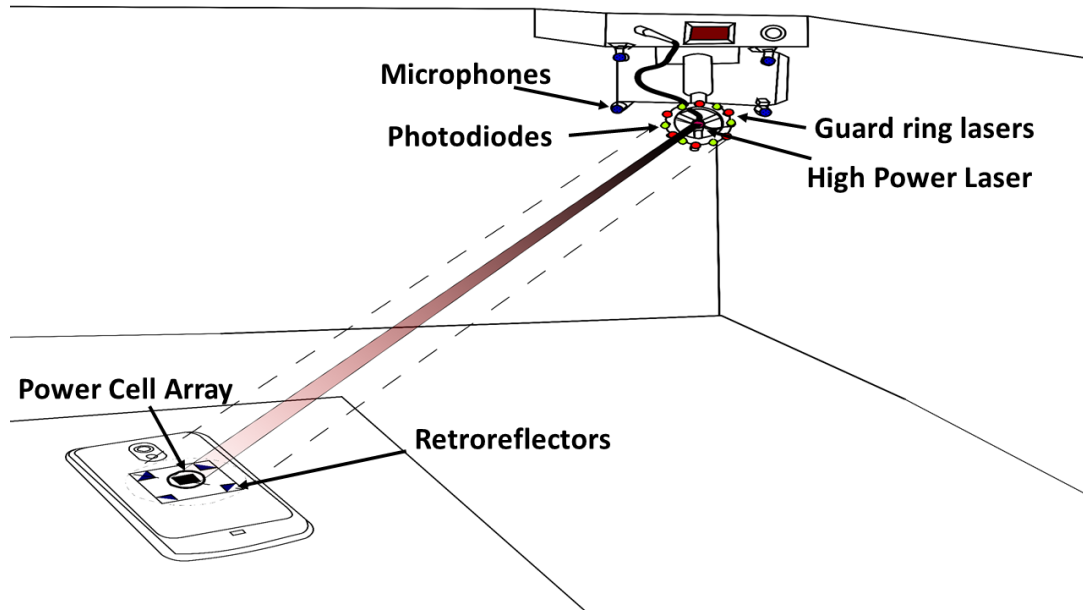
Fig. 4. **System overview.**The laser source has a high power laser, a low-power guard ring laser, microphones for localization and photodiodes to detect the reflections. The receiver has power cells and retroreflectors that reflect the guard ring.

the power is being transferred. Such an approach however is unlikely to work in practice. Assume the power is transferred over a distance $L$, the aperture of the smaller retroreflector is $A$ (this is the one that will be with the device to be charged) and the optical wavelength is $\lambda$. To maintain the lasing, we need to satisfy $\frac{2\pi L}{\lambda} = 2\pi m$, where $m$ is an integer. Intuitively, if the light acquires a $2\pi m$ phase shift as it traverses the cavity and arrives at the same point, it constructively interferes and therefore increases the intensity of the light in the cavity, which is the high level principle behind a distributed optical cavity. This implies that $L$, the separation between the power source and the receiver must be an integer multiple of the wavelength, $L = m\lambda$. To maintain this condition we need to estimate the separation length $L$ with an accuracy of $\left(\frac{\Delta L}{L}\right) \approx \left(\frac{\lambda}{L}\right) \approx 10^{-7} m$ for an optical wavelength of 1 $\mu$m at a distance of 10 m. Moreover, the retroreflector needs to have a stringent angular resolution of at least $\theta \approx \frac{A}{L} \approx 0.001$ rad, assuming $A$ is 1 cm. If we need to have 100 round-trips between the retroreflectors to form the required cavity, we need a resolution of 10 $\mu$rad. Maintaining such stringent spatial and angular resolution requires sophisticated control systems, which would add both power and cost to the power transfer system. While current scientific grade instruments (including piezo-electric controls) can achieve such stringent requirements, as is already done in LIGO (Laser Interferometer Gravitational-Wave Observatory), incorporating piezo-electric control mechanisms significantly increases costs. For example, today a continuous wave laser, with one meter mirror separation costs about $50K [17]. The method proposed in [23], further aims to essentially create a continuous wave laser with ten meters mirror separation, and hence will cost significantly more.

## 3 SYSTEM OVERVIEW
A laser is capable of providing a focused beam with a very high power density. While this allows us to concentrate and direct power to a specific receiver, the power density within the beam exceeds safe limits for humans. Limits for laser safety are based on maximum permissible exposure (MPE) values which is the exposure time below

which a laser of a particular power density has negligible effect on the human eye. These numbers are typically chosen to be 10% of the dose with a 50% probability of damage to the eye [15]. The MPE limits are specified for different wavelength ranges in order to account for the various ways that light can interact with the eye. For example lasers in the visible range can cause retinal burns while higher wavelength infrared (IR) lasers can cause corneal burns. While the eye is most sensitive to damage, a high power laser can also cause skin burns. In order to deliver 1 W of power to a device, assuming even a high conversion ratio of 23% optical to electrical power, would require a 4.3 W laser. For a beam size of 1 $cm^2$, this would be a power density of 4.3 $W/cm^2$ and therefore the corresponding MPE limit for a near IR laser would less than 10 $\mu$s.

Given these constraints and the definition of these exposure limits, we set a goal of designing a system which will prevent *any human exposure to the high power beam.* In order to build such a system that is safe, we need to address two main questions: 1) How do we detect human motion approaching the path of the high power beam and 2) How do we, with minimal delay, turn off the high power laser before the human intersects with it?

**Detecting motion approaching the beam.** Ideally we would like to detect motion orders of magnitude faster than a few microseconds in order to meet the end-to-end delay constraint. Additionally, we would like a solution that adds minimal hardware to the receiver in order to keep a small form factor and prevent having to power an additional device. We analyze possible naïve solutions below:

- *Camera.* One possibility for detecting a person approaching the high power laser beam is to use a camera and computer vision algorithms designed to recognize objects entering the beam area. While this approach may seem intuitive considering we must have line of sight to the receiver, typical cameras have frame rates on the order of 30-60 fps meaning that the sampling rate of the camera alone introduces a delay on the order of milliseconds. Even a high speed 1000 fps camera, which would add significant cost to the system, would still have a 1 ms delay. Assuming the processing pipeline for the vision pipeline adds negligible delay, which is currently not true, this is still significantly longer than required for ensuring safety.

- *Acoustic tracking.* Recent work on acoustic tracking has demonstrated the ability to detect human motion with high accuracy [28]. Unfortunately acoustic methods are inherently limited by the speed of sound (340 m/s) in air, which means that for an acoustic wave to travel from the transmitter to an object even 1 m away introduces a roundtrip delay of almost 6 ms which disqualifies this approach.

- *Power detection and RF communication.* Another approach would be to monitor the amount of power at the receiver itself and send this information back to the laser source via RF communication. If any object comes within the line of sight path between the transmitter and receiver it will block some of the optical power and therefore reduce the electrical power available at the receiver. This value can then be transmitted back using a radio such as Wi-Fi and Bluetooth. This approach is attractive in terms of adding minimal extra hardware to the system, however it suffers from a number of significant limitations. Firstly, this requires that the person actually enter the high power beam unlike the previous approaches which can have a larger field of view. Secondly, the radio interface will add latency to the system — the network delay for sending a Wi-Fi packet is on the order of milliseconds because of contention on the wireless medium.

Our design instead looks to optics, which operates at the speed of light. We create low power lasers to create a guard ring around the high power laser and direct them at retroreflectors on the receiver. The retroreflectors provide a feedback signal we then measure using photodiodes at the transmitter. Considering the round-trip for an optical wave at a distance of 10 m is only 60 ns and photodiodes introduce negligible delay for detection [34], this allows us to build a motion detection system that operates on the order of nanoseconds. Additionally, we introduce a spatial separation between the guard beam and the high power laser which we size ensure that we turn off the high power beam before a human can ever enter it.

**Turning off the beam.** After detecting that there is a person approaching the path of the high-power beam, we need a shutter to turn off the beam quickly. We use an electronic shutter which has maximum delay of 247 *us*
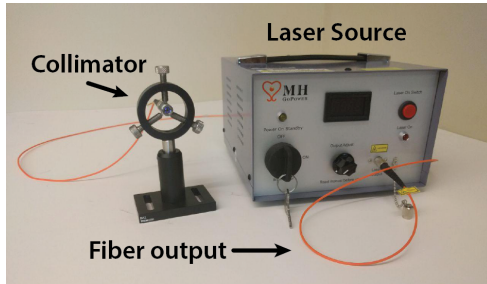
Fig. 5. **Laser Source.** Our high power laser source produces a fiber output for direct connection to optical components. The fiber is connected to a collimator to produce a focused beam in free space.
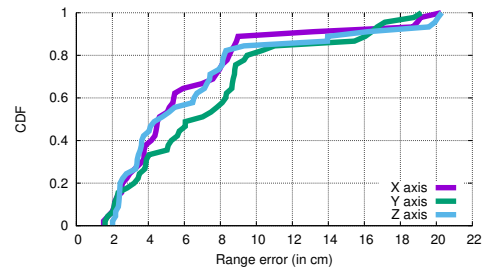


Fig. 6. **Acoustic localization accuracy.** The figure plots the CDF of the localization errors of the smartphone along all the three axes when it was placed at a distance of 12.2 m from the device.

to turn off the laser. While this delay is longer than the maximum permissible exposure (MPE) time above, we can still use this shutter to build a safe system. Specifically, we leverage the fact that the maximum speed of articulated human motion is 44 m/s [36] in throwing motions for professional sports and is fundamentally limited by the force that human joints can tolerate. Based on this speed, assuming a person has already accelerated to this maximum velocity, the maximum a human could ever move within this time duration is 1.2 cm. Therefore, we simply need to detect the approaching human by leaving at least 1.2 cm between the high power laser and the low power guard beam. When the amount of reflected power of the low power guard beam from the retroreflectors decreases, we detect an approaching obstruction and turn off the high power beam before being exposed.

## 4 DESIGN AND IMPLEMENTATION

Our system has two key components: the power source and the receiver. We describe the design and implementation of each of these two components.

### 4.1 Power Source Design

Fig. 4 shows the components in our power source. We explain each of these components in detail.

*1) High-power laser source.* To build our laser power system we use the MHGoPower LSM-010 976 nm laser source which incorporates a laser diode and control system. In order to meet our target of 1 W power delivery, we select a laser capable of outputting up to 10 W of power. Assuming a receiver efficiency of approximately 25%, this allows for extra headroom to account for attenuation versus range and other losses. We select a wavelength of 976 nm as it is not visible to humans but will still work with silicon components such as photovoltaic cells.

*2) Collimator.* Our laser source is designed for use in power over fiber systems and provides a fiber output with a core diameter of 105 $\mu m$. However the output of the fiber does not produce a focused beam necessary for transmission in free space. To do this we connect the fiber output to a collimator shown in Fig. 5, which focuses the light into a narrow beam in free space. In our system we use the Thor Labs F220FC-980 collimator.

An ideal collimator should produce a beam with a constant width regardless of range, however in practice a beam will diverge in space. While laser pointers can maintain a beam width of 6 mm at ranges of over 6 m, we note that the output of our collimator diverges noticeably in space. This is likely due to focusing optics internal to the laser source module. In order to correct for this we test a custom design consisting of multiple lenses with adjustable separation. Using this setup we are able to reduce the beam width from 43 mm to 39 mm at a distance

of 4.57 m, however we observe a lower power output as the components are optimized for broadband operation and ultimately choose to use the F220FC which gives us maximum power output at our wavelength of operation.

*3) Low-power guard beams.* In addition to the powering laser, our safety system requires a low power laser source for the guard beam. This component provides a light source which the retroreflector at the receiver reflects back to the laser source. By using a laser, our feedback system essentially operates at the speed of light. We explore a variety of options for producing the guard ring. At a high level we simply need a light source capable of illuminating the retroreflectors on each side of the receiver. If we take the example of a receiver in the form factor of a phone, our retroreflectors may be placed at the outer edges approximately 7-8 cm apart. One option would be to illuminate all of the retroreflectors with a single wide beam. This can be done by using a combination of a low cost spot laser such as those in laser pointers followed by a beam expander (Thor Labs BE10M-A). This setup has the advantage of minimizing the number of components used, however it adds complexity to the safety system. Since all of the retroreflectors are illuminated by a beam from the same source, we must identify multiple thresholds that correspond to when one or more retroreflectors have been blocked.

As an alternative, we can use a ring consisting of multiple low-power laser beams at the laser source. While this introduces some hardware complexity at the power source, it simplifies the safety system. If each individual laser beam is focused on a specific retroreflector, it will produce a discrete change when blocked. More specifically, by using smaller beams we guarantee that an object moving towards the laser will block the entire beam to a retroreflector thereby producing a guaranteed discrete reduction in the reflected power observed at the photodiode from its maximum value to zero. Additionally, this provides a safeguard against multipath from other objects in the environment. If the entirety of the main beam to the retroreflector is blocked there is no possibility of a reflected signal returning to the photodiode.

*4) Photodiode reflection detection.* The next component in our safety system is reflection detection using photodiodes that receive the reflected laser from the low power guard ring. As explained previously, we wish to minimize the detection delay of our receiver in order to allow the maximum time for the shutter to close, which can be easily accomplished with commercial photodiodes. For example, low cost silicon photodiodes such as the PDB-C156 has a broad spectrum allowing for a variety of wavelengths to be used for the low power guard lasers.

*5) Shutter to turn off laser.* The photodiode signal controls the next component in the system which is the shutter that actually turns off the high power laser. Based on laser safety standards [15], for a 1 cm$^2$ beam with 10 W power at 976 nm, the exposure time should be less than 1 $\mu$s. We can relax this constraint slightly as the human body will move at some finite velocity and therefore take some time to move into the path of the high power beam. Based on the fastest human motion of 44 m/s [36], a gap of 1.2 cm between the guard beam and high power beam allows for 272 us to turn off the high-power laser. We explore multiple options to achieve such a shutter.

- **Mechanical shutters.** A mechanical shutter is the simplest way to block a high power laser beam as it operates by physically blocking the aperture of the laser. Mechanical shutters provide a reliable and low cost means of achieving 100% extinction of the beam. The fastest published mechanical shutter uses a voice coil actuator to achieve sub-microsecond fall times. While this solution appears to be attractive due to its fast fall time, it also has latency of 2 ms or more from the beginning of the control signal sent to close the shutter and full beam extinction. This arises from basic physics as the shutter begins at rest and must first accelerate before it achieves its maximum velocity. Blocking a 1 mm beam within 200 us would require a constant acceleration of 50,000 m/s, which is roughly the same order of magnitude as a bullet.
- **Liquid crystal shutters.** Liquid crystal shutters utilize the same technology as LCD displays with essentially a single large pixel. A liquid crystal shutter consists of the liquid crystal material sandwiched between two orthogonal polarizers. The liquid crystal material introduces an additional 90 degree polarization change therefore allowing light to pass through; however when an electric field is applied to the liquid

crystal it produces no polarization change and light reflected back by the second polarizer causing it to appear opaque. While these shutters have the advantage of no mechanical parts, they typically introduce some attenuation. For example [32] allows a maximum 85% transmission, and still takes 400 $\mu$s to close.
- **Acousto-optic modulators.** An acousto-optic modulator (AOM) is a device, which can pulse the laser or alter the transmitted power at a very high frequency. They function by sending the laser beam through a crystal, which is subjected to acoustic vibrations. These vibrations alter the refractive index of the material, so the beam can be redirected from the output aperture to a beam dump in a very short time. The rise/fall time is limited only by the amount of time it takes for the acoustic wave to traverse the width of the crystal, so this is usually on the order of nanoseconds. While an AOM based shutter can more than meet our timing requirements, it typically costs over $1,000 which would significantly increase the cost of the whole system.
- **Electro-optic modulators** An electro-optic modulator (EOM, also sometimes called a Pockels cell) is similar to an AOM except that it uses an electric field rather than an acoustic wave in order to change the optical properties of the material inside. The Pockels cell inside the EOM alters the polarization state of the beam, and a polarizer is used at the output to convert this change in polarization to a change in amplitude. Because the device uses electric fields rather than mechanical acoustic waves, it can operate faster than an AOM, however it even more expensive.

To achieve our goal we instead control the power supply of the laser. As explained above, the optical output power of a laser depends on the current supplied to the laser diode. By using an electronic switch to turn off the power supply we can turn off the beam. For our specific laser system, we control the power supply electronically using the built in interlock feature. The interlock on our laser source consists of a jumper which must be connected to enable the laser's power source. To electronically control the interlock, we use an MTP2955 MOSFET [38] as a switch to connect and disconnect the two exposed pins. We measure the total delay of this shutter from maximum to minimum power to be 272 us. While this value itself is significantly higher than the MPE time, as described earlier, we introduce the spatial separation between the guard beam and the high power beam to account for this. We note that the speed of 44 m/s assumed for this distance calculation provides a very high upper bound for practical scenarios as 44 m/s corresponds to maximum instantaneous arm motion in professional sports.

*6) Acoustic localization.* Before we begin transmitting power to the receiver, our power source must first determine where in space it is so that it can direct the beam appropriately. A naïve approach would be to scan our low power guard lasers across the room until our photodiodes detect a reflected signal; this is however a time consuming process and would require the transmitter to be constantly scanning. Instead, we propose a joint acoustic-optical localization approach. In our system the device such as a smartphone initiates the charging sequence by transmitting an acoustic signal from its speaker to an array of microphones at the transmitter. We then leverage acoustic localization techniques [28] to determine its coarse location. We then get a finer resolution by using optical components to search in a much smaller space than a whole room.

Our laser power source has four microphones. The speaker at the smartphone transmits a single high frequency chirp signal (8-14 kHz) for 10 ms with a repetition frequency of 9 chirps per second. We choose this frequency range as it is well within the range of most commercial speakers and microphones, but is still above the typical low frequency ambient audio signals such as human speech, fans etc. The chirps are recorded by each of the microphones. The 4 condenser microphones [41] are connected to a Motu MK3 Ultralite audio interface which records each channel concurrently at a sampling rate of 48 kHz.

At the microphone end, we first use a bandpass FIR filter to remove the ambient noise in the recorded signal. We then correlate the transmitted signal with the filtered signal to identify the time of arrival from the receiver to the source. The correlation results in multiple peaks corresponding to the different multipaths between the smartphone and the receiver (similar to [28]). We isolate the line-of-sight path, by identifying the first correlation peak and therefore the shortest path, that crosses a minimum threshold. Since the smartphone and the

receivers are not time synchronised, we cannot measure the exact time of flight of the signal at each microphone. Instead, we compute the time difference of arrival (TDOA) of the chirp signal between the microphones. We then apply multilateration to determine the 3D location of the phone. Specifically, we use a non-linear least squares technique in which we apply gradient descent on the residual error between individual distance difference estimates constrained by the geometry of the room.

We test this localization technique in a large 12 by 30 m room in an office building. The microphone setup along with the MOTU receiver were connected to a laptop and placed in one corner of the room to record the signals. A Samsung Galaxy S4 smartphone running an Android application playing the 10 ms chirp was placed 12.2 m from the microphone setup. The recorded signals were processed on the connected laptop and error between the estimated 3D location and ground truth location was computed along all the three axes. We then repeated this experiment at different angles with respect to the microphones. Fig. 6 plots the localization errors of the smartphone for this experiment. The figure shows that we can localize the smartphone within an average error of 5 cm along each axes at the maximum range. The accuracy of this system is sufficient as it achieves a similar resolution as our laser's beamwidth at this distance.

After determining the position of the receiver, we then attempt to direct our low power lasers at the retroreflectors until we receive a reflected signal at the photodiodes, using techniques from free-space optical communication. We do this by reflecting the beam off of a series of 2 mirror mounted on a servo motors. By controlling the angle of the servo motor we can steer the beam to the desired angle. Because our transmitter will be mounted on the ceiling, we use the first mirror to steer the beam to the appropriate downward angle, and use the second mirror to move the reflection across the room to the correct point.

## 4.2  Receiver Design

The receiver consists of an array of photovoltaic cells that perform the conversion from optical power to electrical power. The output is then connected to a DC to DC converter which provides a 5V output capable of charging smartphones or other USB devices. The physical structure of the converter also incorporates a heatsink to dissipate waste heat as well as the retroreflectors required for the safety system.

*1) Photovoltaic cell.* A photovoltaic cell is a semiconductor device that converts light to electrical energy. In principle, we could use a standard solar panel, however the PV cells in typical solar panels are designed to harvest energy from the broad spectrum of visible light rather than optimized for performance at the specific wavelength of our laser source. Additionally, the cell must be able to tolerate a high power density as the laser beam is a focused source of optical power. So we explore PV cells designed for power over fiber systems as a solution considering these are optimized for receiving high intensity light at a specific wavelength from a laser. Specifically, we use a silicon based vertical multi-junction PV cell (MH GoPower MIH VMJ PV cell). Unlike a typical PV cell, it consists of a sequence of serially interconnected p-n junctions, which are bonded together to form a small PV array with low series resistance, thus achieving performance that does not decrease at higher intensities. Specifically, we select a 1 $cm^2$ VMJ PV cell (MH GoPower 5S1010.4). The cells have an anti-reflective coating in order to minimum loss from power reflected off of the cell.

We note that since the PV cell is composed of an array of sub-cells in series, performance is limited by the outermost junctions. The result of this is that the cells perform best when light over the cell is uniform. The beam from our transmitter however is a circular Gaussian beam in which the intensity peaks at the center and decreases at the outer edges. We find experimentally that at intensities up to 5.5 $W/cm^2$ the cells achieve their maximum power output when operating at 20 V. To convert this to a 5 V output for charging a smartphone, we connect the output to an MP1484 DC-DC step down converter which produces a 5 V output with 95% efficiency.

*2) Retroreflectors.* Our receiver also incorporates retroreflectors to reflect the low power laser beam as our feedback system. A retroreflector is a passive object that ideally reflects light back to its source with minimal scattering and

(a) Ideal corner cube retroreflectors.
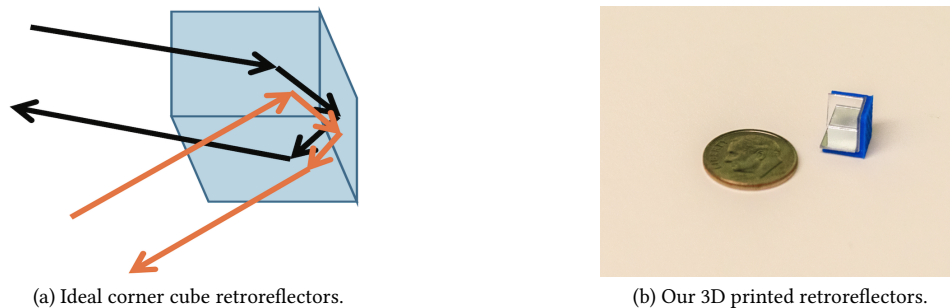


(b) Our 3D printed retroreflectors.

Fig. 7. **Optical retroreflectors.** (a) A corner cube retroreflector reflects incoming light back in the same direction it arrived and (b) We fabricate 6 mm corner cube retroreflectors by attaching plastic mirrors to the interior of a 3D printed structure.

180 degrees reflection angle. For example, as seen in Fig 7, the structure of three mirrors arranged perpendicularly to each other in a corner forms such a retroreflector. For the regular flat-panel mirror, the reflected light is parallel to its incident light if, and only if, the mirror is perfectly orthogonal to the input beam. However, for a retroreflector mirror, the reflected light is parallel to its incident counterpart regardless of its angle of incidence. Retroreflectors are commonly used in safety clothing, road signs, bicycle reflectors, as well as for precision distance measurements.

We experiment with a variety of commercially retroreflective materials such as tapes, and plastic reflectors for road signs as these fit our required small form factor profile well. We found however that these retroreflectors do not have the same behavior as the ideal corner cube. Specifically, we note that these are constructed from arrays of small prisms. While they do produce a reflection back along the same direction, we note that the reflected beam diverges significantly when compared to an ideal corner cube retroreflector. Additionally, we find that these retroreflectors have a limited field of view and do not operate beyond 45 degrees. This is important for our application scenarios considering our laser source will be mounted on a high shelf or ceiling in order to maximize coverage of a room. Assuming the transmitter is mounted on an 2.43-3.04 m ceiling and the receiver is placed flat on a 1 m high table at distances upto 6.09 m, the angle of incidence on the reciever will be between 90–14 degrees. To operate at this range within the small form factor we desire for a phone receiver, we design and fabricate our own corner cube reflectors as shown in Fig. 7(b). Because of its symmetric structure, an ideal corner cube reflector will operate across a wide range of angles where at the extremes it simply becomes a flat mirror. To do this we 3D print an 8 mm corner cube structure using ABS plastic and attach plastic mirrors to each of the three inner faces.

We evaluate our retroreflectors and find that they produce a reflection back in the direction of the beam at the necessary ranges; however we also observe that the reflected beam diverges similar to the plastic commercial retroreflectors we tested previously. This beam divergence is due in part to the spreading of the beam across the round trip path from the laser source, but mostly due to the roughness at the edges of the reflector due to our fabrication method. We evaluate this spreading of the beam and demonstrate that we can still receive enough reflected power at our transmitter to detect when the beam has been blocked.

*3) Heat dissipation.* The bare cell can only operate for 5 s at maximum power after which its temperature exceeds 125 °C and its efficiency drops to near zero. We examine a variety of options for heat dissipation below to allow long term stable operation. Considering the phone charging case has the most stringent form factor constraints, we focus the analysis below on this case. A larger charging surface such as a table could use the same techniques.

- **Flat plate heatsink.** The simplest heatsink design is a flat metal plate. In the case of charging a phone, this is an attractive solution considering it can be made thin and flat to fit on the back of a phone. We attach the cell in the center of a flat rectangular piece of 0.5 mm thick copper using a layer of Arctic Thermal 5 thermal paste between the layers. This design extends the operating time of the cell at max power from 5 s

(a) Heatsink diagram



(b) Heatsink prototype

Fig. 8. **Heatsink assembly.** The PV cell is attached to a thermoelectric generator using thermal adhesive and mounted on an aluminum heatsink allowing the cell to output a stable 1.3 W for 8 hrs.

to about 15 min, which is still not a feasible solution. We choose copper due to its high thermal conductivity, however copper is also very electrically conductive and would cause the metal contacts on the back of the cell to short. To address this we place a layer of kapton tape which can tolerate high temperatures at under the edges of the cell as an electrical insulator. While this allows the cell to function, it increases the thickness of the thermal interface layer between the cell and the heatsink. Considering the conductivity of thermal pastes is two orders of magnitude less than, this layer dominates the thermal resistance.

- **Active cooling.** We also explore options for actively cooling the device in order to maintain a low operating temperature. Devices such as fans and thermoelectric coolers can both be very effective thermal management solutions when combined with a heatsink. A fan provides air flow which makes convection the dominant mode of heat transfer from the metal heatsink to the air. Convection is significantly more efficient than radiation and therefore greatly improves cooling performance. While fans provide a simple and effective method for cooling, they consume significant amounts of power and space. For example a small 35 x 35 mm fan adds an additional 6 mm of thickness above a heatsink and consumes 200 mW of power. Thermoelectric coolers provide another means of active cooling. These devices take advantage of the thermoelectric effect. When heat is applied between two differently doped semiconductor materials, the temperature gradient causes diffusion of charge carriers and creates a voltage difference. The effect works in reverse as well and by providing a voltage across the device induces a temperature difference. The advantage to a thermoelectric cooler is that it can be made relatively thin to fit the form factor of a phone, however the trade off is these coolers have low efficiencies which reduces the power available for charging.

Our final design uses a combination of heatsink with fins as well as a thermoelectric generator. Specifically, we mount the cell on an 4.5 mm thick aluminum heatsink [40] with 2 mm tall fins and a 100 $u$m thick thermal adhesive as the interface layer. Although the thermal adhesive is conductive, we cut away the sections that would come into contact with the metal pads on the cell to prevent it from shorting. While aluminum has a lower thermal conductivity than copper, we note that the adhesive or thermal paste layer still dominates the thermal resistance of the system. Additionally, a heatsink with fins allows greater air flow through the device. This design keeps the cell operating at maximum power for over 2 hours. We note that the temperature increases and reaches a steady state after approximately 1.5 hrs after which the temperature and electrical output are stable.

Since our system produces a significant amount of wasted heat, we use a thermoelectric generator (TEG) to harvest some of this heat. We modify the design above to add a thermoelectric generator. We mount the cell onto one side of a thermoelectric generator [13] using a 100 um thick layer of Arctic Alumina Thermal Adhesive. On the opposite side we attach the aluminum heatsink described above. Fig. 8 shows our prototype. To shield users from the high temperature of the heatsink and cooler, we place the assembly in a 1 mm thick 3D printed case made of ABS plastic and covered with an additional insulating layer of kapton tape.

(a) Full transmitter and receiver setup  (b) Transmitter  (c) Receiver
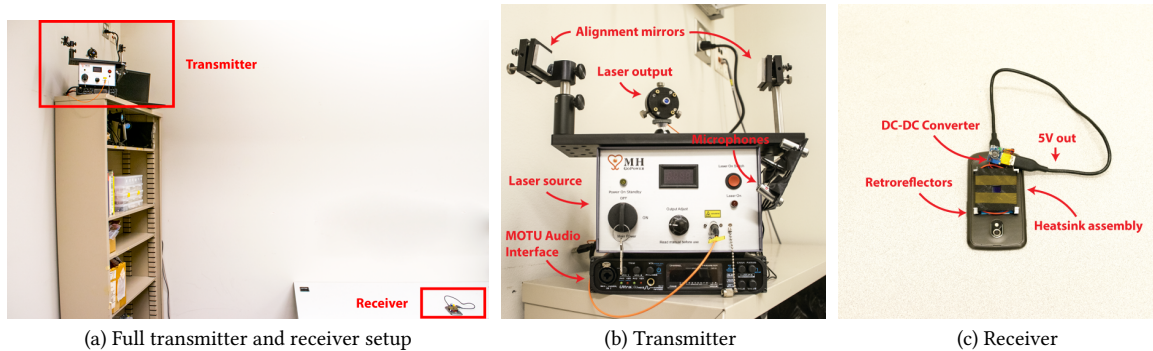
Fig. 9. **Evaluation setup.** (a) Full system with the transmitter on a shelf aimed down at a receiver. (b) The transmitter including the laser source, microphones, audio interface, and manual alignment mirrors used to direct the beam during experiments. (c) Receiver assembly in a plastic case with retroreflectors shown with a smartphone for scale.

## 5 EVALUATION

In this section we evaluate each component of our system motivated by a series of practical performance and safety questions. The first question we evaluate is the safety of our design. Next, we ask how much power our system can deliver while operating within the constraints needed for safety. Finally, we perform experiments to determine whether our system can maintain a consistent power output over an extended period of time.

### 5.1 How safe is the system?

We evalute two key safety metrics in our design: reliability, delay and reflected laser power.

**Reliability.** As described earlier, the safety of our system is ensured by the retroreflectors that provide a feedback mechanism to trigger the shutter, whenever a human approach the path of the high-power laser. In order to operate reliably, the retroreflector must provide a feedback signal across the distance to the power source with sufficiently high SNR to trigger the shutter.

To evaluate this, we measure the amount of reflected power from the retroreflector using a photodetector at the transmitter for different distances. We set up a scenario similar to our intended use case where our laser power source would be mounted on the ceiling or placed on a high shelf while receivers such as phones or tabletops will be placed on flat surfaces parallel to the ground as seen in Fig 9. Specifically, we place a low-power 5 mW 635 nm laser pointer on a shelf at a height of 1.52 m above the floor. For a typical 2.43-3.04 m ceiling, a 1.52 m clearance allows the receiver to be placed on a surface such as a table typically 0.6-1 m high. We direct the laser pointer at a mirror (Edmund Optics) with a precisely adjustable angle. We place the retroreflector on an 8 mm thick piece of cardboard on the floor simulating the thickness of a smartphone or other device to be charged. We move the retroreflector along the floor to different distances. We point the laser at the retroreflector and measure the power of the reflection with an optical power meter (Thor Labs S121C).

Fig. 10 shows the result of sweeping across a range of 6.09 m. The plot shows that the difference between the reflected power in the presence and absence of an obstruction is significant. More specifically:

- As the distance increases the angle of incidence at the retroreflector changes as well. At the minimum distance, the beam begins at 90° with respect to the floor, and decreases to 15° at the maximum range. This shows that the retroreflector has a wide enough field of view for use at long ranges. Additionally, because the corner cube is symmetric, this also demonstrates that the retroreflector is relatively invariant to changes in orientation as a retroreflector should be.
- While the reflected beam does return along the same path, the size of the beam increases significantly due to divergence of the original laser beam roughness of the inner joints of the manually fabricated cube. The
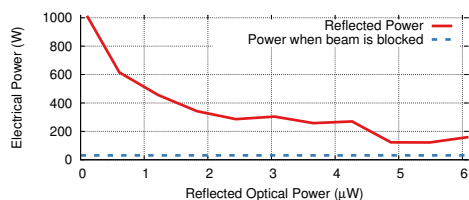
Fig. 10. **Retroreflector range.** The plot shows the power of the light reflected back from our 6 mm retrore-flectors as observed at the source's photodiodes. The figure also shows results in the presence of blockage.
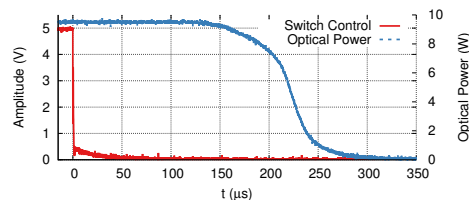


Fig. 11. **Shutter timing.** Timing diagram showing the shutter response time beginning at $t = 0$ when the control signal is given to 272 $\mu$s when the high power laser beam is completely off.

reflected beam as it is not perfectly circular and reflects the texture at the edges of the retroreflector. The effect of the beam spreading is a lower received power density and therefore a lower photodiode output.
- Despite the spreading of the beam, the reflected power remains high enough for detection across the whole range. We compare this to measurements from the photodiode when line of sight to the retroreflector is obstructed which averages 31 $\mu$W on our power meter. Even at the minimum reflected power of 122 $\mu$W (which is observed at a distance of 6.09 m) this still gives us an SNR greater than 5 dB, allowing us to reliably detect obstructions.

**Delay.** In addition to having a sufficient SNR from the reflected signal, we also need to minimize the delay in turning off the laser source. There are multiple components that contribute to this delay. At a distance of 12.2 m, the round trip laser delay is around 80 ns. The second component is the photodiode at the laser source which adds a few microseconds as described earlier. The delay is dominated by how quickly we can turn off the high power beam after detecting the guard beam has been blocked. To characterize the delay between activating the shutter and reducing the beam power to a safe level, we apply a control signal from an ATMEGA328 microcontroller to turn off the laser. While applying the control signal we measure the output power of the laser using the same power meter after passing through an 20 dB attenuator. We record these signals on a Tektronix MDO4104 oscilloscope and plot the results in Fig 11.

Our results show the following:

- The controller for the laser's power source introduces some latency. We can see there is a period of 100 $\mu$s following the control signal when there is no change in the output power of the laser. Following this time, the fall time of the power itself is 172 $\mu$s.
- The rise time of the digital control signal introduces a negligible delay on the order of nanoseconds.
- The total time it takes for the beam to go from the maximum power of 9.5W to 0 is 272$\mu$s. This timing determines the spacing required between the guard beam and the high power laser. Considering the fastest possible human motion is 44 m/s [36], the maximum a person could move within this 272 $\mu$s is 1.2 cm. Therefore, by leaving at least 1.2 cm between the high power laser and the low power guard laser, we can ensure that a human will never be exposed to the high power beam.

**Reflected Power.** The above safety system can eliminate the high power beam when a person walks directly into it, but reflections of the high power laser must also be considered while evaluating safety. We note that our design satisfies two key properties. First, the high power beam is always in line of sight to the receiver. Second, since the high power laser beam in our design, is contained within the array of photodiodes at receiver, reflections of the high power laser only occur around the surface of the photodiodes and power converter at the receiver. In order to evaluate this we measure the reflections off of our power converter at different angles. While the high power laser is on, we use the same power meter as before and place it at angles from 30° to 60° facing the
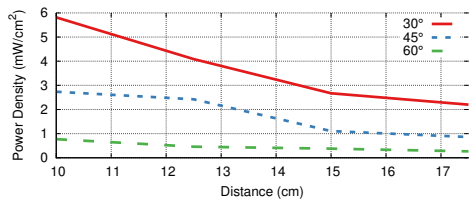
Fig. 12. **Reflected light from power converter.** Reflected power measured at varying angles and distances from the power converter demonstrating reflections of the high power laser are not harmful.
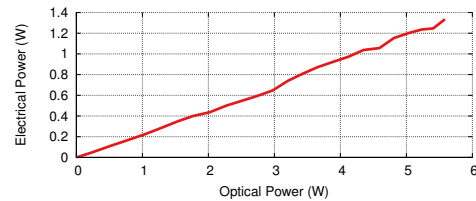


Fig. 13. **PV cell efficiency.** Conversion efficiency of our PV cell showing how much optical power is converted to electrical power.

power converter. At each angle we took measurements at a height parallel to the beam, as well as above and below at several ranges. Based on the raw power measurements we calculate the average power density and plot the results versus range from the power converter in Fig. 12.

The figure shows that even at a distance of 10 cm from the power converter, the reflected power density is below $6 \ mW/cm^2$ across the whole range of measured angles and distances meaning it is safe for eye exposure [15]. We can see that going beyond this distance the power density decreases even further as expected.

### 5.2 How much power can we receive?

Now that we have demonstrated our safety system is capable of preventing harmful exposure to our high power laser, we next evaluate how much power we can actually receive. To do this, we first measure the efficiency of our power converter with a single photocell. We then evaluate the amount of spreading that the beam undergoes with distance. Finally, we evaluate the two case scenarios of charging a phone form factor device and delivering power to a table top.

**Converter efficiency.** We place our power converter 1.3 m away from the collimator and orient it such that the converter surface is orthogonal to the direction of the beam. At this distance, the circular collimator output fully covers the 1 cm² receiver. Because the power converter consists of multiple photovoltaic cells connected in series, its performance is limited by the outermost subcells. Making the beam slightly larger than the cell achieves maximum power. Additionally, as described earlier, using a circular beam makes the system invariant to changes in orientation of the cell. We connect the power converter to a variable DC load (HP6036B) which maintains the cell voltage at 20 V at which it achieves maximum power output. We use a multimeter to measure the current and calculate the total power output of the cell. To determine the optical power actually incident on the cell, we use calipers to measure the beam diameter at this distance to be 14.64 mm. We use this value to determine the power density and use the input power to the cell to calculate efficiency in Fig 13.

The figure shows that a single cell achieves an average 23% efficiency for converting optical power to electrical power. This is at least 5-10% greater than typical silicon solar cell efficiencies [43], and can further be improved by increasing the uniformity of the beam over the cell using a diffuser or other optical components. We note that the maximum electrical power in Fig 13 is limited by the output power of our laser over the area of the cell.

**Beam spreading.** Next we evaluate the range at which we can feasibly transmit this power. Our maximum range is determined by two factors: the attenuation of the laser beam itself in air, and the size of the beam at the receiver. Ideally, a collimated laser should produce a beam which maintains a constant width as it propagates through space. However in practice the beam typically expands and diverges depending on the optical components used. A laser pointer [2] with an 3 mm aperture for example can produce a beam width of 6 mm at 6.1 m. However the laser and collimator we use in our system produce a more noticeable divergence. To evaluate the divergence of our collimator, we use calipers to measure the beam diameter versus range. We perform this experiment in a
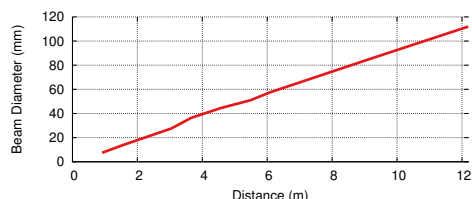
Fig. 14. **Beam divergence.** This plot characterizes the spreading of the beam versus distance.
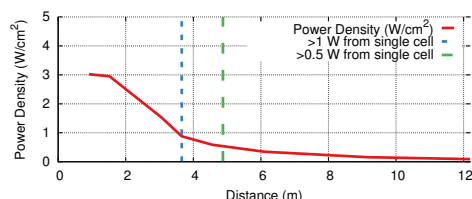


Fig. 15. **Power density versus range.** Power density decreases versus range as the beam diverges.

normal office environment with no precautions taken to minimize dust. Fig 14 shows the results, and we note that at 5.5 m the beam is ≈50 mm wide, and increases to 100 mm at 12.2 m.

In addition to the size of the beam, we also measure the attenuation of the beam through air. While the beam should experience no attenuation in vacuum aside from spreading due to the beam divergence, in real environments dust particles can also cause attenuation. We measure the power of our laser output from the collimator using an optical power meter placed at the center of the beam in a normal office environment at ranges up to 12.2 m. As the beam spreads, it becomes larger than the 20 mm single power detector aperture. We therefore plot the power density measured over the power meter. Fig 15 shows the power density varies as a function of distance. Additionally, because our PV cells are 1 cm² this plot also shows the maximum electrical power that can be received by a single cell at a particular range. According to Fig 15, a single cell can provide greater than 1 W at distances up to 3.65 m, and over 0.5 W up to 4.87 m.

**Charging a phone.** Because we wish to maintain a distance of around 1 cm between our low power guard beam and the high power beam for safety, our range becomes constrained by a combination of this beam divergence observed above and the form factor required by our application. In the case of the iPhone 7 plus, which has a 78 mm width, allowing space for our retroreflector and 12 mm on either side for the guard distance allows a maximum beam width of 42 mm. Designing within the constraints of this form factor allows us the flexibility to extend the system to IoT devices as well which are approximately the same size.

According to the beam divergence measurements in Fig. 14, this corresponds to a maximum range of 4.27 m. Because we cannot guarantee safety beyond this point, we first use our localization system to determine whether the phone is within this safe operating range before allowing the high power laser to be switched on. Fig 15 shows that a single cell can produce greater than 1 W of electrical power at a range up to 3.66 m.

While the power density of the beam at longer ranges such as 5.48 m is lower than necessary to receive 1 W of power using a single cell, this is only capable of harvesting power from a small fraction of the total beam. By using an array of power converters we could collect the power available over the whole beam area. In the case of the iPhone 7 plus, which has a 78 mm width, allowing space for an 13.9 cm² array of photocells, our 6 mm retroreflectors and 1.2 cm guard distance. This supports a maximum beam width of 42 mm and therefore a maximum operating range of approximately 4.3 m as shown in Fig 16. Below this limit, we can see there is sufficient optical power over this whole range to support power transfer above 2 W. Beyond this distance, however, we turn off the laser source since we cannot guarantee the safety since the high power beam would larger than the size of the phone and hence our guard beams cannot be reflected by the retroreflectors.

**Delivering power to a tabletop.** Next we examine the case of a tabletop, in which the beam may be significantly larger than the previous 42 mm limitation that is enforced by the size of a smartphone. To understand how much power is available we apply the same method by combining the beam area with the measured power density to determine the total optical power available. Fig 17 shows the available optical power with a photocell array that covers a 100 cm² area. This plot demonstrates that by increasing the size constraints on the receiver, we can
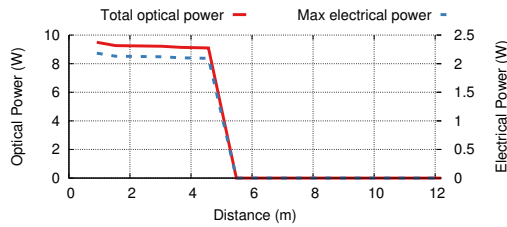
Fig. 16. **Delivering power to a smartphone.** We deliver more than 2 W up to a distance of 4.3 m.
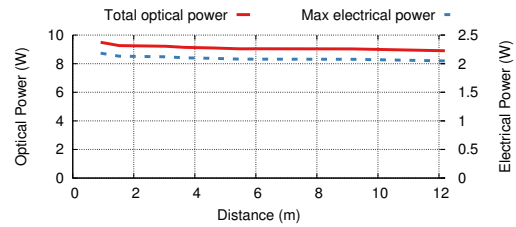


Fig. 17. **Delivering power to a tabletop.** We can deliver 2W at more than 12.2 m.

provide over 2 W of electrical power across the whole range of 12.2 m within the room. Additionally, the table form factor also relaxes the constraints on the size of the retroreflector, and we demonstrate that using our same low power laser we receive a 195 uW reflection using a 50 mm retroreflector prism (Thor Labs PS976). Fig 17 also confirms that the attenuation through air is insignificant and the range could be further extended if necessary; we choose to limit our range measurements up to 12.2 m as this is more than sufficient for coverage of very large rooms in indoor environments while still maintaining a beam diameter roughly twice the width of a smartphone.

### 5.3 How long can we run the system?

Lastly, we verify that our system can provide a continuous, reliable power source for an extended period of time. The primary factor affecting the output power over time is the temperature of the device. Because the power converter is only 23% efficient, a significant amount of power is converted into heat. Although the cell itself may be able to tolerate a high temperature, the efficiency of the cell decreases quickly at high temperatures. To demonstrate this, we show the output power of a bare cell exposed to the maximum power. We use the same collimator setup described earlier and place a bare cell at a distance of 1.3 m from the laser output oriented orthogonal to the beam direction. We increase the optical power until the maximum and plot the received electrical power in Fig 18.

Fig 18 shows that the bare cell is only able to output power for 5 s after which it reaches a temperature of 150°C. To verify that our final heatsink design described in our design section is capable of stable operation, we perform an experiment over the course of 8 hrs and measure both the electrical output power from the converter as well as the outer temperature. The latter is not only a concern for maintaining high efficiency power transfer, but also for safety; our laser safety system prevents exposure to the high power laser however if the power converter on the back of the phone is allowed to reach high temperatures it also presents a safety risk.

We place the power converter and heatsink in the same configuration described above used to test the cell efficiency. We place the converter at a distance of 1.3 m from the collimator orthogonal to the direction of the beam. We then connect the output of the converter to a variable DC load to maintain it at 20 V and use a multimeter to monitor the current. Additionally, we incorporate a thermoelectric generator (TEG) into our design as described previously in order to convert some of the waste heat into usable electrical energy. We connect the output of the thermoelectric generator to a 2.3 Ω resistor to match its impedance and use a multimeter to measure the current produced by the device. We turn on the laser to the maximum power output and allow the system to run for the full 8 hrs taking intermediate measurements of converted power from both the laser power converter and the thermoelectric generator, as well as temperature using an IR camera (FLIR E4).

Our results can be summarized as follows.

- After approximately 15 min the power values appear to settle to a steady state varying by only a few degrees for temperature while the current only fluctuates by a few milliwatts. This remains constant for the remainder of the 8 hr period showing this system is capable of providing a reliable power source.
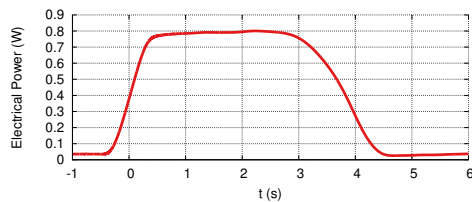
Fig. 18. **Power without the heatsink.** The bare cell can only operate for 5 s since it heats up to 150°C.
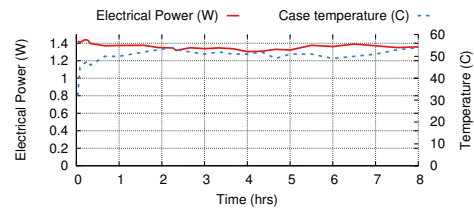


Fig. 19. **Power versus time.** Our design operates for more than 8 hours and delivers a watt with a single cell.

- The average temperature of the ABS plastic casing settles to an average of 51°C, going up to a max of 54°C. This is well within the safety limits for plastic casings of consumer products [16]; the exterior enclosure will be noticeably warm as with a typical phone charger, but will not be hot enough to pose a safety threat.
- Fig. 19 shows the system is capable of producing an average of 1.36 W of electrical power, from a single photocell, over the duration of our 8 hr experiment reaching a minimum of 1.304 W.
- Up until 2 hrs the temperature increases steadily to a steady state of approximately 50°C, and the electrical power decreases slightly. While there are some changes in power after this point that appear to be correlated with temperature, there are other periods that are not. This is caused by fluctuation in the power of the laser as we observe in other experiments that the output power can vary by up to 200 mW.
- The thermoelectric generator produces an average of 4 mW. This low output is expected as the efficiency of these devices is typically on the order of 1%. This may be marginally increased by improving the thermal interface between the cell and the surface or by using an energy harvesting chip that performs maximum power point tracking in order to maintain the optimal load resistance.

## 6 DISCUSSION AND CONCLUSION

We provide the first end-to-end wireless power solution capable of safely transmitting power across a whole room and give extensive characterization supported by empirical data demonstrating that our system will never expose a human to a harmful high power laser. We discuss a number of possibilities to improve our system.

**Safely delivering higher power.** The power levels presented in this work are limited by our specific hardware implementation and are not fundamental to our techniques. For example, our maximum power transfer is only limited by our laser source as the PV cells are designed to handle even higher power densities. Scaling up the power does however present some challenges such as the need for an improved heatsink. This presents an opportunity to explore interesting performance trade-offs such as if active cooling using a fan or thermoelectric cooler can enable a high enough total power that the fraction used by the cooling device becomes insignificant. Our range for charging sized constrained devices such as phones could be significantly improved using a different collimator and focusing elements and is not limited by attenuation as shown in Fig. 17.

**Improving the delay.** Our safety system can also be further improved to reduce the time required to close the shutter or reduce the latency between activating the shutter and when it begins to turn off the laser. Laser drivers capable of producing microsecond pulses [8] to reduce the separation between the high power beam and the guard beam in order to increase the useful area over which we can harvest power.

**Leveraging optical metasurfaces.** Researchers have demonstrated planar retroreflectors [3] that we could leverage these techniques to create flat lenses, or other optical elements to produce a uniform beam across the cell. Additionally recent work on optical antennas [35] suggests potential for improving the efficiency of our PV cell. Finally, because we use a laser source unlike broadband light harvested by typical solar cells we could use a cavity enhanced photodiode designed to operate efficiently at a particular wavelength of light.

**Powering low-power sensors and devices.** In addition to scaling up this concept to support high-power devices, we could also scale back this system for lower power devices. Specifically, many IoT sensors are designed for low power duty cycled operation. A single laser source could therefore be used to sequentially power and query these sensors. This could be especially useful in industrial applications in which a single power access point could act as a hub for powering and collecting data from sensors across large spaces such as warehouses. Making these sensors battery free could significantly increase their lifetime and decrease maintenance costs.

**Line-of-sight limitation.** We note that one major constraint on our system is that it requires line of sight for operation, and we could not for example charge a phone in a user's pocket. We consciously make this decision however considering a single line of sight path provides the strongest safety guarantees and we can always prove the system is safe rather than having to account for complex multipath in changing environments.

**Concurrently powering multiple devices.** One could also explore methods of simultaneously powering multiple receivers. In the simple case of two devices, this could be accomplished using a 50% beam splitter which simply splits the output power between two paths. In order to simultaneously support additional receivers, one could leverage techniques that use spatial light modulators or digital micromirror devices (DMD) to create complex diffraction patterns with multiple output beams [11].

## ACKNOWLEDGMENTS

## REFERENCES

[1] M. C. Achtelik, J. Stumpf, D. Gurdan, and K. M. Doth. 2011. Design of a flexible high performance quadcopter platform breaking the MAV endurance record with laser power beaming. In 2011 IEEE/RSJ International Conference on Intelligent Robots and Systems. 5166–5172. https://doi.org/10.1109/IROS.2011.6094731

[2] Adafruit. 2017. Laser diode- Red. (2017). https://www.adafruit.com/product/1054

[3] Amir Arbabi, Yu Horie, and Andrei Faraon. 2014. Planar Retroreflector, In CLEO: 2014. CLEO: 2014, STu3M.5. https://doi.org/10.1364/CLEO_SI.2014.STu3M.5

[4] Hal E Bennett. 1995. DOD and Navy applications for laser power beaming. SPIE Laser Power Beaming II Proceedings (1995).

[5] Michael Buettner, Richa Prasad, Alanson Sample, Daniel Yeager, Ben Greenstein, Joshua R. Smith, and David Wetherall. 2008. RFID Sensor Networks with the Intel WISP. In Proceedings of the 6th ACM Conference on Embedded Network Sensor Systems (SenSys '08). ACM, New York, NY, USA, 393–394. https://doi.org/10.1145/1460412.1460468

[6] Matthew J. Chabalko, Mohsen Shahmohammadi, and Alanson P. Sample. 2017. Quasistatic Cavity Resonance for Ubiquitous Wireless Power Transfer. PLOS ONE 12, 2 (02 2017), 1–14. https://doi.org/10.1371/journal.pone.0169045

[7] Shane S. Clark, Jeremy Gummeson, Kevin Fu, and Deepak Ganesan. 2009. Towards Autonomously-Powered CRFIDs. (2009).

[8] IXYS Colorado. 2015. PCO-6141. (2015).

[9] Energous. 2017. (2017). http://energous.com/

[10] USB Implementers Forum. 2004. USB 2.0 Standard. (2004). http://www.usb.org/developers/docs/usb20_docs/

[11] Monia Ghobadi, Ratul Mahajan, Amar Phanishayee, Nikhil Devanur, Janardhan Kulkarni, Gireeja Ranade, Pierre-Alexandre Blanche, Houman Rastegarfar, Madeleine Glick, and Daniel Kilper. 2016. ProjecToR: Agile Reconfigurable Data Center Interconnect. In Proceedings of the 2016 ACM SIGCOMM Conference (SIGCOMM '16). ACM, New York, NY, USA, 216–229. https://doi.org/10.1145/2934872.2934911

[12] Brent Griffin and Carrick Detweiler. 2012. Resonant wireless power transfer to ground sensors from a UAV. In Robotics and Automation (ICRA), 2012 IEEE International Conference on. IEEE, 2660–2665.

[13] Ltd Hebei I.T. (Shanghai) Co. 2001. TEC1-12706. (2001). http://peltiermodules.com/peltier.datasheet/TEC1-12706.pdf

[14] E Hoffert, P Soukup, and M Hoffert. 2004. Power Beaming for Space-Based Electricity on Earth: Near-Term Experiments with Radars, Lasers and Satellites. In Solar Power from Space-SPS'04, Vol. 567. 195.

[15] IEC 60825-1 2001. Safety of Laser Products. Standard. International Electrotechnical Commission.

[16] IEC 60950-1 (2005) 2005. Information technology equipment âĂŞ Safety. Standard. International Electrotechnical Commission.

[17] Coherent Inc. 2017. In Private communication.

[18] Ossia Inc. 2017. (2017). http://www.ossia.com/

[19] André Kurs, Aristeidis Karalis, Robert Moffatt, J. D. Joannopoulos, Peter Fisher, and Marin Soljačić. 2007. Wireless Power Transfer via Strongly Coupled Magnetic Resonances. Science 317, 5834 (2007), 83–86. https://doi.org/10.1126/science.1143254 arXiv:http://science.sciencemag.org/content/317/5834/83.full.pdf

[20] Hyeonseok Lee, Hyun-Jun Park, Hoon Sohn, and Il-Bum Kwon. 2010. Integrated guided wave generation and sensing using a single laser source and optical fibers. Measurement Science and Technology 21, 10 (2010), 105207.

[21] Summerer Leopold and Oisin Purcell. 2009. Concepts for wireless energy transmission via laser. Europeans Space Agency (ESA)-Advanced Concepts Team (2009).

[22] James C Lin. 2006. A new IEEE standard for safety levels with respect to human exposure to radio-frequency radiation. IEEE Antennas and Propagation Magazine 48, 1 (2006), 157–159.

[23] Q. Liu, J. Wu, P. Xia, S. Zhao, W. Chen, Y. Yang, and L. Hanzo. 2016. Charging Unplugged: Will Distributed Laser Charging for Mobile Wireless Power Transfer Work? IEEE Vehicular Technology Magazine 11, 4 (Dec 2016), 36–45. https://doi.org/10.1109/MVT.2016.2594944

[24] Vincent Liu, Aaron Parks, Vamsi Talla, Shyamnath Gollakota, David Wetherall, and Joshua R. Smith. 2013. Ambient Backscatter: Wireless Communication out of Thin Air. In Proceedings of the ACM SIGCOMM 2013 Conference on SIGCOMM (SIGCOMM '13). ACM, New York, NY, USA, 39–50. https://doi.org/10.1145/2486001.2486015

[25] Yunxin Liu, Zhen Qin, and Chunshui Zhao. 2015. AutoCharge: Automatically Charge Smartphones Using a Light Beam. (2015).

[26] KA Unnikrishna Menon, Achyuta Gungi, and Balaji Hariharan. 2014. Efficient wireless power transfer using underground relay coils. In Computing, Communication and Networking Technologies (ICCCNT), 2014 International Conference on. IEEE, 1–5.

[27] J. Mukherjee, W. Wulfken, H. Hartje, F. Steinsiek, M. Perren, and S. J. Sweeney. 2013. Demonstration of eye-safe (1550 nm) terrestrial laser power beaming at 30 m and subsequent conversion into electrical power using dedicated photovoltaics. In 2013 IEEE 39th Photovoltaic Specialists Conference (PVSC). 1074–1076. https://doi.org/10.1109/PVSC.2013.6744326

[28] Rajalakshmi Nandakumar, Vikram Iyer, Desney Tan, and Shyamnath Gollakota. 2016. FingerIO: Using Active Sonar for Fine-Grained Finger Tracking. In Proceedings of the 2016 CHI Conference on Human Factors in Computing Systems (CHI '16). ACM, New York, NY, USA, 1515–1525. https://doi.org/10.1145/2858036.2858580

[29] NASA. 2004. Laser power for UAVs. (2004).

[30] Taysir Nayfeh, Brian Fast, Daniel Raible, Dragos Dinca, Nick Tollis, and Andrew Jalics. 2011. High intensity laser power beaming architecture for space and terrestrial missions. (2011).

[31] Thomas J. Nugent, Jr. and Jordin T. Kare. 2011. Laser power beaming for defense and security applications. (2011), 804514-804514-8 pages. https://doi.org/10.1117/12.886169

[32] Meadowlark Optics. 2017. High contrast optical shutter. (2017). http://www.meadowlark.com/store/data_sheet/opticalshutter.pdf

[33] Aaron N. Parks, Angli Liu, Shyamnath Gollakota, and Joshua R. Smith. 2014. Turbocharging Ambient Backscatter Communication. In Proceedings of the 2014 ACM Conference on SIGCOMM (SIGCOMM '14). ACM, New York, NY, USA, 619–630. https://doi.org/10.1145/2619239.2626312

[34] Advanced Photonix. [n. d.]. PDB-C156. http://advancedphotonix.com/wp-content/uploads/PDB-C156.pdf

[35] S. Raavi, B. Arigong, R. Zhou, S. Jung, M. Jin, H. Zhang, and H. Kim. 2013. An optical wireless power transfer system for rapid charging. In 2013 Texas Symposium on Wireless and Microwave Circuits and Systems (WMCS). 1–4. https://doi.org/10.1109/WMCaS.2013.6563551

[36] Jeremy Repanich. [n. d.]. ([n. d.]).

[37] A. Sahai and D. Graham. 2011. Optical wireless power transmission at long wavelengths. In 2011 International Conference on Space Optical Systems and Applications (ICSOS). 164–170. https://doi.org/10.1109/ICSOS.2011.5783662

[38] NXP Semiconductors. 2000. MTP2955. Rev. 4.

[39] Bożena Smagowska and Małgorzata Pawlaczyk-Łuszczyńska. 2013. Effects of ultrasonic noise on the human bodyâĂŤa bibliographic review. International Journal of Occupational Safety and Ergonomics 19, 2 (2013), 195–202.

[40] Advanced Thermal Solutions. 1995. ATS-6000-C1-RO. (1995). https://www.digikey.com/product-detail/en/advanced-thermal-solutions-inc/ATS-60000-C1-R0/ATS1376-ND/1285090

[41] Sony. 2011. Electret Condenser Microphone. (2011). https://images-na.ssl-images-amazon.com/images/I/714s6fjypPS.pdf

[42] F Steinsiek, KH Weber, WP Foth, HJ Foth, and C Schafer. 2004. Wireless power transmission experiment using an airship as relay system and a moveable rover as ground target for later planetary exploration missions. In 8th ESA Workshop on Advanced Space Technologies for Robotics and Automation. 1–10.

[43] Seeed Studios. [n. d.]. 0.5W Solar panel. ([n. d.]). http://wiki.seeedstudio.com/index.php?title=0.5w_Solar_Panel_55*70

[44] Vamsi Talla, Bryce Kellogg, Benjamin Ransford, Saman Naderiparizi, Shyamnath Gollakota, and Joshua R. Smith. 2015. Powering the Next Billion Devices with Wi-fi. In Proceedings of the 11th ACM Conference on Emerging Networking Experiments and Technologies (CoNEXT '15). ACM, New York, NY, USA, Article 4, 13 pages. https://doi.org/10.1145/2716281.2836089

[45] Wibotic. 2017. (2017). http://www.wibotic.com/